Soft Matter

PAPER

View Article Online
View Journal | View Issue

Cite this: *Soft Matter*, 2021, **17**, 2234

Production of giant unilamellar vesicles and encapsulation of lyotropic nematic liquid crystals†

Peng Bao, [a] Daniel A. Paterson, [ab] Sally A. Peyman, [ac] J. Cliff Jones, [a] Jonathan A. T. Sandoe, [c] Helen F. Gleeson, [a] Stephen D. Evans [a] and Richard J. Bushby *[b]

Received 18th September 2020,
Accepted 1st December 2020

DOI: 10.1039/d0sm01684e

rsc.li/soft-matter-journal

We describe a modified microfluidic method for making Giant Unilamellar Vesicles (GUVs) *via* water/octanol-lipid/water double emulsion droplets. At a high enough lipid concentration we show that the de-wetting of the octanol from these droplets occurs spontaneously (off-chip) without the need to use shear to aid the de-wetting process. The resultant mixture of octanol droplets and GUVs can be separated by making use of the buoyancy of the octanol. A simpler microfluidic device and pump system can be employed and, because of the higher flow-rates and much higher rate of formation of the double emulsion droplets (~1500 s^{-1} compared to up to ~75 s^{-1}), it is easier to make larger numbers of GUVs and larger volumes of solution. Because of the potential for using GUVs that incorporate lyotropic nematic liquid crystals in biosensors we have used this method to make GUVs that incorporate the nematic phases of sunset yellow and disodium chromoglycate. However, the phase behaviour of these lyotropic liquid crystals is quite sensitive to concentration and we found that there is an unexpected spread in the concentration of the contents of the GUVs obtained.

1. Introduction

Giant Unilamellar Vesicles (GUVs) have many potential applications.[1–8] They are widely used as cell models (protocells)[9,10] and in studies in which the ultimate aim is to create artificial life.[10–15] As a result, many methods have been developed for their production and for encapsulating materials within them.[16–21] None of these methods are wholly problem-free[22] but microfluidic approaches probably offer most control. Microfluidics allows very small volumes of liquid to be brought together with high spatial and temporal accuracy and so it provides control of both size and uniformity in GUV production.[23–29] Flow-focussed microfluidic methods are based on the production of an intermediate 'double emulsion' (water/oil-phospholipid/water) droplet, Fig. 1a. In the ideal case, if the interfacial tensions at the three interfaces satisfy the inequalities (1)–(3),[29] the oil phase spontaneously de-wets to produce separate oil droplets and GUVs, Fig. 1c.[28,29]

$$\gamma_1 - (\gamma_3 + \gamma_2) < 0 \quad (1)$$

$$\gamma_2 - (\gamma_3 + \gamma_1) < 0 \quad (2)$$

$$\gamma_3 - (\gamma_2 + \gamma_1) > 0 \quad (3)$$

In these equations γ_1 is the interfacial tension between the internal and external aqueous solutions (W1 and W2), γ_2 is the interfacial tension between the oil-phospholipid phase and external aqueous solution (O and W2), and γ_3 is the interfacial tension between the oil-phospholipid phase and internal aqueous solution (O and W1).[29]

The flow-focussed microfluidic method developed by Huck *et al.*[29,30] uses glass capillaries to produce the double emulsion droplets. The 'oil' used is a mixture of chloroform and hexane and de-wetting and formation of the GUVs, occurs post-production (off-chip). The use of chloroform introduces some issues of biocompatibility. The flow-focussed microfluidic method developed by Dekker *et al.*[11,22,28,31–33] uses the more biocompatible 'oil' octanol, the double emulsion droplets are produced in a conventional polydimethylsiloxane (PDMS) microfluidic device and de-wetting and separation of the octanol droplets from the GUVs occurs 'on-chip'. In both of these microfluidic methods, a poloxamer/pluronic surfactant is used to fine-tune the interfacial tensions and to control the de-wetting process. Poloxomer/pluronic surfactants generally have excellent biocompatibility but their interactions with biomembranes is complex[34] and they can, for example, affect bilayer fluidity.[35] In the Dekker group method it also appears that an element of shear and contact with the PDMS walls is needed to aid the de-wetting process. In this paper, we report a modification to the Dekker group method. We show that substantially increasing the lipid

[a] *School of Physics and Astronomy, University of Leeds, Leeds, LS2 9JT, UK*
[b] *School of Chemistry, University of Leeds, Leeds, LS2 9JT, UK.*
E-mail: r.j.bushby@leeds.ac.uk
[c] *Leeds Institute of Medical Research, University of Leeds, Leeds, LS2 9JT, UK*

† Electronic supplementary information (ESI) available. See DOI: 10.1039/d0sm01684e

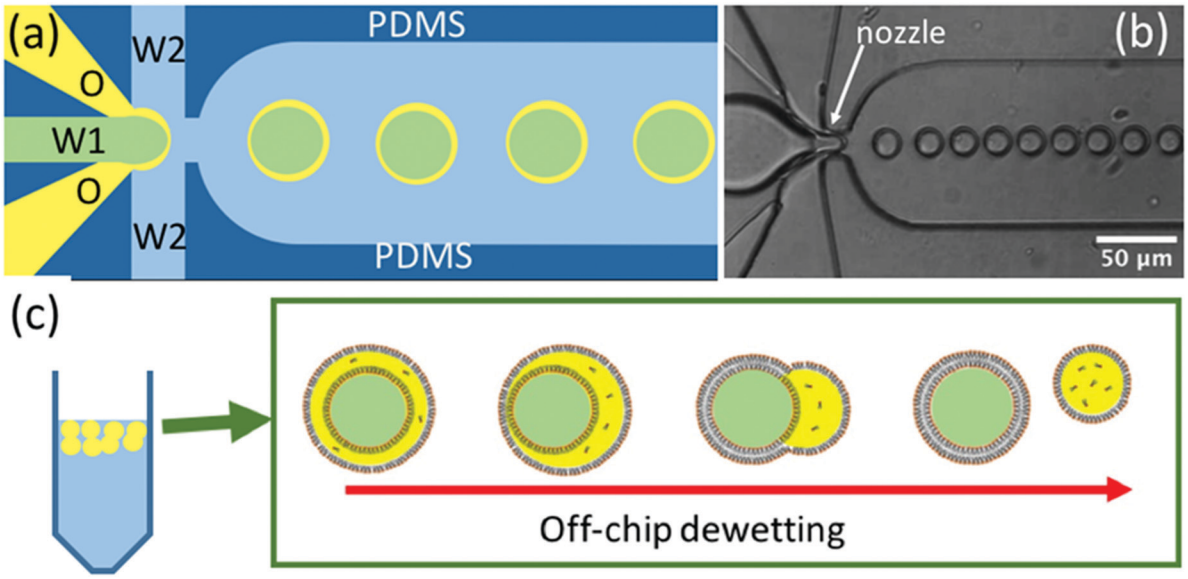

Fig. 1 (a) Schematic diagram of the microfluidic device used for the generation of water/oil/water double emulsion droplets (green: internal aqueous phase W1; yellow: oil (octanol-phospholipid) phase O; blue: external aqueous phase W2). (b) Optical microscopy image of a microfluidic device in use taken with a high-speed camera near the nozzle where the double emulsion droplets are being produced, Video SV1 (ESI†). (c) Schematic diagram of the de-wetting process off-chip, in which the oil phase separates giving a mixture of GUVs and oil droplets.

concentration in the octanol facilitates spontaneous de-wetting and allows the production of GUVs without the need for poloxomer/pluronic surfactant. The production rate of the double emulsion droplets is increased by ~20 times and the separation of the GUVs from the oil droplets is also made much easier (separation is effected off-chip).

Our aim was to enclose lyotropic nematic liquid crystals within the GUVs. The principle of exploiting the responsive nature of thermotropic nematic liquid crystal droplets to create biosensors is already well established.[36–43] These droplets make use of the signal amplification that occurs when a small change in liquid crystal surface anchoring energy results in a large change in the bulk director field. In the simplest case, a change of the anchoring at the liquid crystal/water interface from perpendicular to planar switches the director field from radial to bipolar configurations, Fig. 2a and b.[44] This change produces an optical response that is easy to detect.[45] The use of a phospholipid monolayer to surround these droplets,[36,46] Fig. 2c, provides a natural bridge between the aqueous world of biology and the hydrophobic world of thermotropic liquid crystals and it allows some natural membrane components to be incorporated into the structure. However, most of the natural plasma membrane proteins that would be, at least in principle, useful in creating sensitive, specific biosensors (*e.g.* those involved in analyte recognition, in signal transduction and in signal amplification) only function in a phospholipid bilayer environment. GUVs filled with a lyotropic nematic liquid crystal (LNLC, Fig. 2d) may enable harnessing of the functions of these natural plasma membrane proteins.

The nature of the director fields obtained in LNLC 'droplets' is much less well explored than that of their thermotropic counterparts.[47–50] Differences that are observed arise mainly because of the rather different elastic moduli found in lyotropic systems.[47–50] Although lyotropic liquid crystals are often less

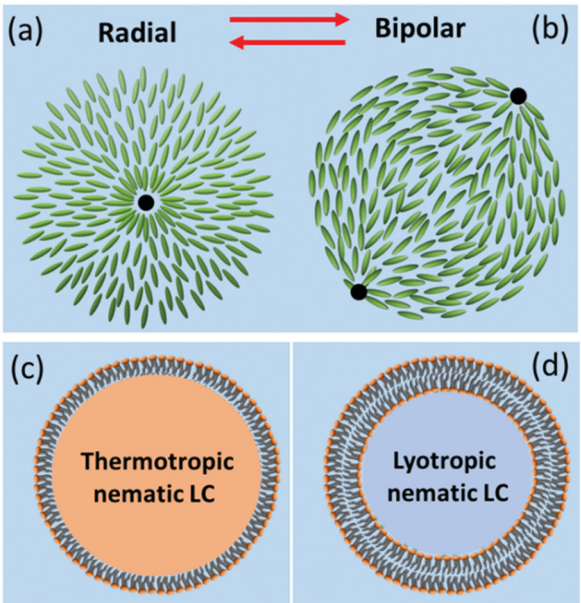

Fig. 2 The two commonest, extreme liquid crystal director fields seen in thermotropic nematic liquid crystal droplets and a schematic of a lipid monolayer or bilayer on thermotropic nematic and lyotropic nematic liquid crystals. (a) Radial director field with homeotropic/perpendicular anchoring of the liquid crystal at the interface, and a three-dimensional hedgehog defect at the centre. (b) Bipolar director field with planar/tangential anchoring at the interface, and two boojum defects at opposing poles. (c) A thermotropic liquid crystal droplet in water surrounded by a phospholipid monolayer. (d) A lyotropic liquid crystal containing GUV in which the outer layer is a phospholipid bilayer.

sensitive to changes in the surface than for thermotropic liquid crystals,[51] their behaviour at this type of interface remains to be explored.

The attempt to incorporate LNLCs in these GUVs was only partly successful because, surprisingly, it was found that the GUVs were not uniform in terms of the concentration of the internal aqueous component. LNLC phases are only stable over rather limited concentration ranges.[52] Diluting the aqueous solution results in a loss of liquid crystal order and a transition from the nematic to the isotropic phase, whereas concentrating the solution results in the formation of a more ordered phase; most often a columnar phase. Lyotropic LCs are particularly sensitive to concentration.

2. Results & discussion

2.1. Modifications to the microfluidic octanol-assisted formation of GUVs

In the octanol-assisted method of forming GUVs introduced by Dekker *et al.*,[11,22,28,31,32] monodisperse double emulsion droplets (water/octanol-phospholipid/water droplets) were produced using a microfluidic device with a flow-focused configuration. When 2 mg mL^{-1} lipid in octanol is used as the 'oil' phase the resultant droplets develop a prominent oil pocket on one side. In this case it seems that the inequalities (1)–(3) are not fully satisfied and that an element of shear, or of interaction with the walls of the channel is required to complete the de-wetting (the channels used by the Dekker group were 11 μm deep for GUVs of 20 μm diameter).[43] This reliance on shear and/or contact with the walls of the channel is possibly the reason for the slow flow rates employed (and slow double emulsion formation rates, 25–75 droplets s^{-1}), and why such precisely controlled device manufacture and pumping systems were originally specified.[22] The GUVs were formed and manipulated on-chip. This has some advantages; for example, on-chip it is possible to split GUVs into two[11] and to produce arrays of trapped GUVs.[32] However, it also has the disadvantage that very long exit channels are required and rather elaborate on-chip systems have to be employed to separate the GUVs from the droplets of oil.[22,31,32]

The main modifications to the procedure that we have adopted were:

(1) The use of deeper channels (*ca.* 25 μm) so that shear interactions and interactions of the double emulsion droplets with the channel walls were reduced.

(2) The amount of lipid in the octanol was increased from 2 to 15 mg mL^{-1} so that de-wetting became a spontaneous process.

(3) The double emulsion droplets thus formed were collected, processed and the GUVs separated from the oil droplets off-chip.

(4) We found that poloxomer/pluronic surfactant was not required to control the de-wetting process.

These changes simplify the chip design and manufacture. Images of the devices that we used are shown in Fig. 1b and in Video SV1 (ESI†). There is no need for the very long channels (which increase the hydraulic resistance in the device) to allow de-wetting to occur nor are elaborate systems needed to accomplish on-chip separation.[22,31,32] Because de-wetting is now an off-chip spontaneous process, the chip dimensions and pressure (pump) control do not need to be as precisely controlled. However, the main advantage of these changes is that the production of the double emulsion droplets is much faster and it is easier to produce larger numbers of GUVs and to produce larger useful volumes of GUV solution. Up to 1500 double emulsion droplets s^{-1} can be produced rather than the original 25–75 s^{-1} and, because the flow rate is ~20 times greater than that originally used, it becomes possible to produce *ca.* 1 mL of a solution of GUVs (10^6 GUVs) within a day from a single chip. Spontaneous separation of the double emulsion droplets into GUVs and oil droplets typically takes 1–3 h. It is then possible to allow the (less dense) oil droplets to rise to the top of the tube and to collect the separated GUV solution by pipette. We found no noticeable decrease in the number of GUVs after a week of storage at room temperature. Because the lipids we normally used were a mixture of DOPC and DOPG (1 : 1 molar ratio) and these GUVs carry negative charges this could help to enhance the stability of the double emulsion droplets/GUVs and to prevent fusion. However, GUVs made using 1 : 1 DOPC : DPPC were found to be just as long-lived.

The double emulsion droplets shown in Fig. 3 were made using 2 mg mL^{-1} of lipid. To aid visualisation, 0.1 mol% of a fluorescent-labelled lipid (Texas Red-DHPE) was also added to the DOPC–DOPG mixture and 0.05 mM calcein (green fluorescence) was added to the internal aqueous solution. The red ring-like structures seen in Fig. 3a arise from the fluorescence of the octanol-lipid layers (the outer shells) of freely-floating water/oil/water double emulsion droplets and the smaller uniform red 'dots' are due to a few remaining octanol-lipid droplets. As shown in Fig. 3b, a strong green fluorescence was observed corresponding to

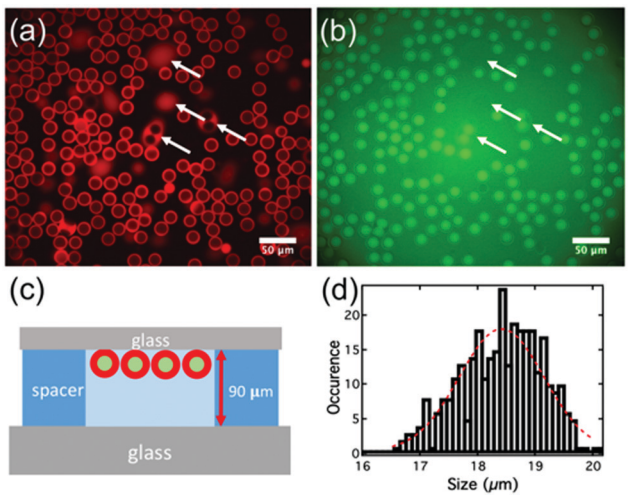

Fig. 3 (a) (False-colour) fluorescence image of the double emulsion using a Texas Red filter; (white arrows indicate double emulsion droplets that have stuck to the glass). (b) (False-colour) fluorescence image of the double emulsion using a fluorescein isothiocyanate (FITC) filter. (c) Schematic of the container used for the imaging of the double emulsion droplets. These are lighter than water and float to the top of the solution. (d) Size distribution for this preparation of the double emulsion droplets.

the encapsulated calcein. However, a green fluorescence was also observed from the external solution. This could be due either to leakage of internal solution when the double emulsion was being formed or due to the break-up of some of the double emulsion droplets during the observation. The apparent thin green shells observed in Fig. 3b are due to the lensing effect of the calcein fluorescence from the background solution. The double emulsions produced are monodisperse (PDI = 0.0026). For this sample the distribution of the sizes can be fitted with a Gaussian function with the peak located at 18.4 μm and a half width at half maximum of 1.1 μm, Fig. 3d.

When the concentration of lipid in octanol was 2 mg mL^{-1} the double emulsion droplets did not de-wet, but, when the lipid concentration was increased to *ca.* 15 mg mL^{-1}, a spontaneous de-wetting process occurred. Collected samples examined shortly after preparation showed mostly double emulsion droplets that had begun to de-wet but which had large oil droplets still attached to their sides, Fig. S2 (ESI†). However, after ~3 h the de-wetting process was complete. The less dense oil droplets rose to the top of the solution. Although not essential, separation is made even easier if there is a density difference between the GUVs and the surrounding medium. Hence, if the GUVs contain sucrose solution and the medium is an equal molarity solution of glucose, the GUVs sink to the bottom.[53] The GUVs can then be removed using a pipette, Fig. 4c. Typical images obtained using the epifluorescence microscope are shown in Fig. 4a and b. The red fluorescence due to the labelled lipid shows as a fairly homogeneous ring which is much narrower than that seen for the double emulsion droplets (compare Fig. 3a and 4a). As in the original work on octanol-assisted GUV formation,[22,31] we found that, for some of the GUVs, de-wetting was imperfect and one or more very small droplets of octanol could be seen in the bilayer. The presence of these small residual droplets is not always easy to see in 'still' images but it is very clear when the GUVs are tumbling in solution, Video SV2 (ESI†). For the particular sample of GUVs shown in Fig. 4 the distribution of the sizes can be fitted with a Gaussian function with the peak located at 9 μm and the half width at half maximum of 1.5 μm (PDI = 0.020), Fig. 4d. This is not quite as good as the size distribution reported by Dekker, wherein GUVs of width 5.6 ± 0.6 μm, 10.8 ± 0.5 μm, 15.9 ± 0.7 μm and 19.5 ± 0.7 μm were obtained.[28] The size of the double emulsion droplets and that of the GUVs can be controlled by controlling the flow-rate.[28]

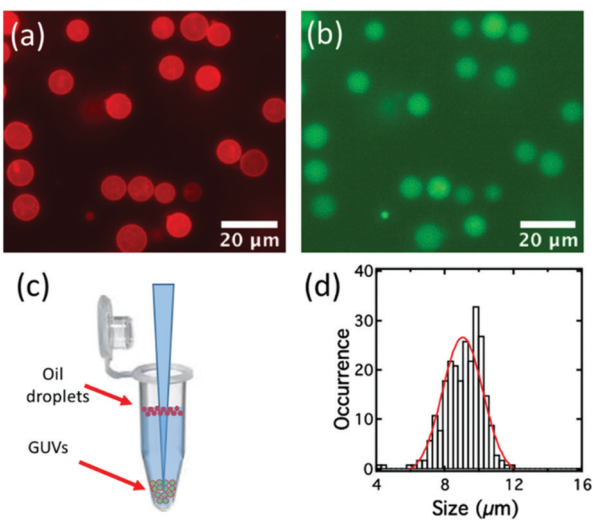

Fig. 4 (a) (False-colour) fluorescence image of the GUVs under a Texas Red filter. (b) (False-colour) fluorescence image of the GUVs under FITC filter. (c) Schematic of the separation of GUVs at the bottom of an Eppendorf tube from the oil droplets floating on the surface of the solution. (d) Size distribution for a typical sample of GUVs. These GUVs were produced under the same conditions as the double emulsion droplets shown in Fig. 3 except with 15 rather than 3 mg mL^{-1} of lipid so that spontaneous de-wetting occurred.

As in the original study, it was shown that alpha-hemolysin initiates the leakage of the calcein. We showed that, when the channel-forming protein (alpha-hemolysin) was added to the external aqueous solution this inserts into the bilayer and after *ca.* 1 min, the intensity of the fluorescence signal from the calcein in the GUVs started to drop reaching the background level in *ca.* 5 min, ESI† Fig. S3 and Video SV2.[28]

2.2. The production of GUVs encapsulating a LNLC

For the production of GUVs that enclose a LNLC, there are a number of mesogens that could be used. We have used two of the most widely studied and best-characterized systems: solutions of sunset yellow (SSY)[54,55] and of disodium chromoglycate (DSCG)[56,57] in water.

SSY in water show a narrow nematic range (*ca.* 28–34 wt%) at 20 °C but the nematic phase persists up to *ca.* 90 °C, Fig. 5a. Solutions of SSY in its LNLC phase were too viscous to use in the microfluidic system. However, a 7 wt% (isotropic) solution of SSY could be used and the double emulsion droplets formed underwent the usual spontaneous de-wetting process to produce GUVs. It was found that the lifetime was longer when 1% glycerol was used as the external aqueous solution[60] rather than glucose or sucrose solution (the aqueous solutions that were used in all our other experiments). By increasing the concentration of glycerol in the external medium it was then possible to shrink these GUVs[30] using osmosis. An image of the GUVs (diameter 19.0 + 1.8 μm) at the beginning of the shrinking process is shown in Fig. S5 (ESI†) and one after shrinking using 15% glycerol is shown in Fig. 6a. As the GUVs shrank and the concentration of the SSY rose there was a transition from the isotropic phase to a liquid crystal phase and they became birefringent. Starting with a 7% solution of SSY, formation of a nematic phase requires a *ca.* 75–80% decrease in volume and a 37–42% decrease in diameter, assuming that the GUVs remain spherical, Fig. 7. However, although the GUVs formed by 'osmotic shrinking' were birefringent, most were oval/tactoid shaped.[61] Under crossed polarizers these GUVs were bright when at an angle but dark when their long axes were aligned with the direction of polarization. This is the kind of behaviour that is consistent with a nematic liquid crystal with a bipolar director field, Fig. 2b,[49] but it is likely that these objects contain SSY in its columnar phase[62] (compare Fig. 6a with Fig. 2b shown by Zimmermann *et al.*[56]). This would require a >81% decrease in volume of the GUV. Fig. 6a shows that there was also a smaller number (*ca.* 12% of the total sample)

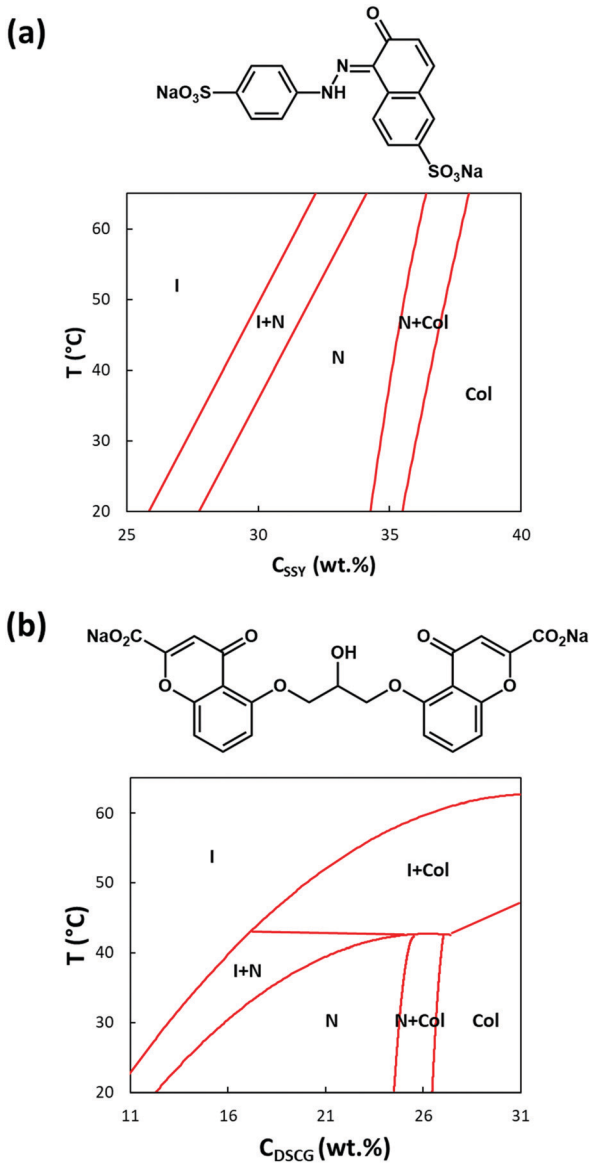

Fig. 5 (a) Phase diagram and Chemical formula for SSY in water (phase diagram redrawn from Joshi *et al.* and Park *et al.*[58,59]) (b) Phase diagram and Chemical formula for DSCG in water (phase diagram redrawn from Zimmermann *et al.*[56]) I = isotropic solution, N = nematic phase, Col = columnar phase.

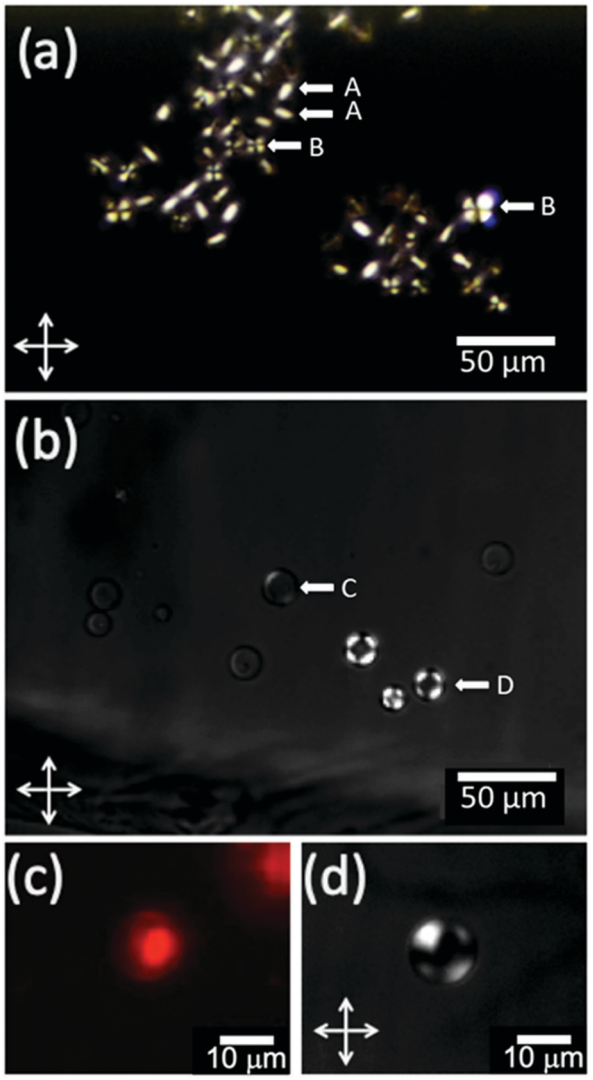

Fig. 6 GUVs loaded with solutions of SSY (7%) and DSCG (12%). (a) Polarised optical microscope (POM) image of GUVs enclosing liquid crystalline SSY solutions. Some of these (A) are oval/tactoid and probably contain SSY in its columnar phase whist others (B) are round and contain the nematic liquid crystal. (b) POM image of GUVs enclosing the isotropic (C) and nematic phases (D) of DSCG solutions. (c) Fluorescence image of a GUV enclosing the nematic phase of aqueous DSCG showing both the lipid membrane and a residual droplet of octanol. (d) POM image of the same GUV.

of more round GUVs that certainly contained the nematic phase. These showed the 'Maltese Cross' pattern typical of a LNLC with a radial director field. The lifetime of these GUVs was short (maximum two hours).

Disodium chromoglycate (DSCG) in water exhibits a relatively wide nematic phase range at 20 °C, spanning the concentration range between *ca.* 12 and 24.5 wt% and the nematic phase persists up to *ca.* 43 °C,[56] Fig. 5b. It shows good biocompatibility and it has previously been used in several bio-related studies.[63,64] Also, the nematic phase is sufficiently non-viscous to use directly in the microfluidic system. However, it was found that the problem with DSCG-based systems is that there is rapid swelling of the double emulsion 'droplets'. This happens over a wide range of conditions and concentrations, even when, on the basis of the measured osmolarities of the solutions, Fig. S4 (ESI†), they should have shrunk. An example of this swelling of the droplets is shown in Video SV5 (ESI†). In Fig. S5 (ESI†) the diameter of one of these droplets is plotted as a function of time. Over one hour, its diameter increased by 90%, which corresponds to a 590% increase in the volume and an 85% decrease in the concentration of the DSCG. In this case, the aqueous phase on the outside of the double emulsion droplet was 1.2 M sucrose and inside the double emulsion droplet the DSCG solution was initially 15 wt%. Based on measured osmolarities, these double emulsion droplets should have shrunk, not swollen. To obtain GUVs containing aqueous DSCG in its nematic phase it was found that

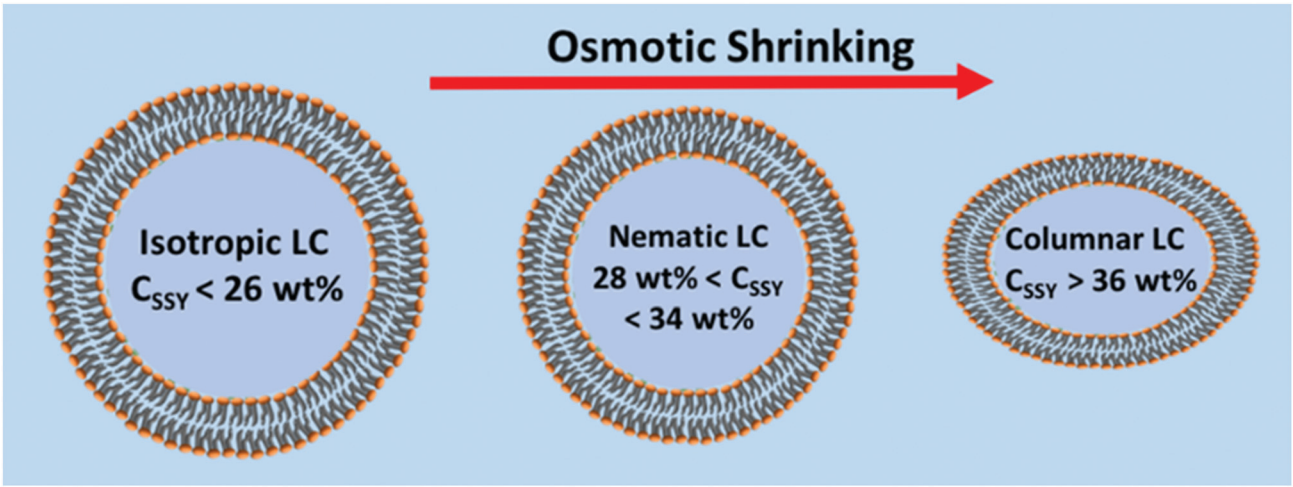

Fig. 7 Schematic of the effect of osmotic shrinking on GUVs containing SSY solutions: how the phase is expected to change at 20 °C as the GUV shrinks in size, as the osmolarity of the external solution is increased. Between the isotopic and nematic phase, and also between the nematic and columnar phase there are concentration ranges in which the two phases co-exist.

the de-wetting needed to be rapid. This was achieved by further increasing the lipid concentration to 30 mg mL^{-1}. This decreased the time taken for de-wetting to about 20 min. This was successful but (compared to the GUVs filled simply with an aqueous solution) de-wetting was not as clean. Many more of the GUVs formed showed very small droplets of residual octanol in the bilayer and sometimes several small droplets. Examples of the DSCG solution-loaded GUVs made in this way are shown in Fig. 6c and d and a residual small pocket of oil is clearly visible in Fig. 6c. Under polarized microscopy with crossed-polarizers, a Maltese Cross pattern was observed, which is typical of a radial director field, Fig. 6d. This alignment of the DSCG aggregates perpendicular to the surface is similar to that reported for droplets of 6.4 wt% DSCG solution in 10.9 wt% PVA (MW ~ 89–98 K) in water (water in water emulsions).[48] However, it is opposite to the alignment reported by Abbott *et al.* for DSCG in GUVs made with a mixture of a PC and pegylated lipid where alignment is found to be planar.[61]

Although alignment of lyotropic nematic liquid crystals is generally less responsive to changes in the surface (most surfaces) than their thermotropic counterparts, at lipid surfaces the nature of the lipid is clearly important. It would also be interesting to explore the relationship between the ordering of the LC and the size of the GUVs. We expect that there will be a lower size limit beyond which the radial director field is no longer possible due to the elastic forces, and an upper limit when the unilaminar structure breaks down. However, in this study we have only explored a roughly two-fold range of sizes. Even when using 30 mg mL^{-1} of lipid in the octanol and rapid de-wetting, swelling remained an issue. Only some of the GUVs formed were birefringent. Others were non-birefringent and presumably contained DSCG solution in its isotropic phase. Furthermore, if the sample was observed over a period of a few hours the birefringent (nematic) GUVs slowly converted to non-birefringent (isotropic) GUVs so that eventually only a few remained in which the DSCG solution was still in its nematic phase. Eventually, all of the DSCG-containing GUVs became isotropic. This loss of birefringence could be due either to swelling of the GUVs or loss of DSCG through the bilayer. A swelling sufficient to cause a change from nematic to isotropic phase could be associated with a change in diameter of only 1–2%, which would be undetectable by optical microscopy.

The swelling of the double emulsion droplets and of the GUVs containing DSCG was not simply due to the mismatch in osmolarity between the two aqueous solutions, Fig. S4 (ESI†). Rather it seems to be due to some specific interaction between DSCG and octanol (perhaps the higher solubility of DSCG in octanol) and it is certainly related to having both octanol and DSCG present. Hence, when double emulsions were produced using oleic acid as the oil phase rather than octanol, although they did not de-wet to form GUVs, they did not swell. Those droplets were stable over a 12 h period. On heating these double emulsion droplets, a transition of the DSCG solution from the nematic to the isotropic phase was observed and the nematic phase reappeared on cooling. As may be seen in Video SV4 (ESI†), when the solution was heated from 10 °C to 50 °C and observed using crossed polarizers, although some of the droplets became isotropic at about the expected temperature of 26 °C, (for this 12 wt% solution) they did not all become isotropic until the temperature was 41 °C, (the transition temperature expected for a *ca.* 16 wt% solution).

3. Conclusions

Through modification of the octanol-assisted microfluidic method for GUV production, it is possible to make larger numbers of GUVs and to make larger volumes of GUV solution without the need to use shear or to add poloxamer to aid their production. Chip design is simplified and only 'standard' pumping systems are required. There is no need for slow flow-rate pumps or for secondary pumping systems to aid on-chip de-wetting. It is possible to

incorporate the LNLC phases of SSY and DSCG within these GUVs. One can envisage biomolecule detector systems being based on such GUVs, which either make use of the switching of the anchoring of the LNLC between perpendicular and planar or which make use of phase changes in the lyotropic liquid crystal. However, before this becomes practicable, this study shows that many issues need to be overcome. Some of these were expected, such as the issue of the viscosity of the LNLC solutions and the need to control the osmotic balance between the contents of the GUV and the surrounding medium. However, some unexpected phenomena were also encountered such as the swelling of the DSCG-containing double emulsion droplets and GUVs. The more fundamental challenge that this study revealed however, is that, although double emulsion droplets and GUVs made by octanol-assisted de-wetting only show a small spread in size, they have quite a significant spread in terms of the concentration of their contents. This is evidenced by the observations that –

(1) The SSY-containing GUVs produced by osmotic shrinking are a mixture of types: probably a mixture in which the contents are in the nematic phase and those in which they are in the columnar phase, Fig. 6a.

(2) The DSCG-containing GUVs are also a mixture of types: a mixture in which the contents are in both the nematic and isotropic phases, Fig. 6b.

(3) The DSCG-containing (oleic acid) double emulsion droplets show a significant spread in the nematic to isotropic transition temperature on heating, Video SV4 (ESI†).

(4) The uneven rates of swelling of the DSCG-containing (octanol) double emulsion droplets leading to a significant spread in the time taken to reach the nematic to isotropic transition, Video SV5 (ESI†).

Assuming that there is no mixing of the two aqueous phases (W1 and W2 in Fig. 1a) during or prior to formation of the double emulsion droplets this spread in concentrations could arise from passage of either water or DSCG/SSY through the octanol-lipid layer in the double emulsion droplets or through the lipid bilayer of the GUVs. From the standpoint of producing a sensor system, the fact that there is this range of concentrations, is a major problem. However, within the wider context of assessing different methods of making GUVs, this study also shows that the sensitivity of LNLCs to concentration makes them excellent 'markers' for testing control over the concentration of the contents.

Conflicts of interest

The authors declare no conflict of interest.

Acknowledgements

The authors gratefully acknowledge the financial support from EPSRC (UK) with grant no: EP/P024041/1. SDE is also supported by Health Services and Delivery Research Programme, Grant/Award Number: MIC-2016-004 and MRC: MR/M009084/1. RJB, SDE, and SAP also wish to acknowledge support from the EPSRC EP/P023266/1. JCJ is supported from EPSRC for a Fellowship in Manufacturing EP/S029214/1.

References

1 T. Robinson, P. Kuhn, K. Eyer and P. S. Dittrich, *Biomicrofluidics*, 2013, **7**, 44105.
2 M. Yoshida, E. Muneyuki and T. Hisabori, *Nat. Rev. Mol. Cell Biol.*, 2001, **2**, 669–677.
3 T. Baumgart, A. T. Hammond, P. Sengupta, S. T. Hess, D. A. Holowka, B. A. Baird and W. W. Webb, *Proc. Natl. Acad. Sci. U. S. A.*, 2007, **104**, 3165.
4 Y. Inaoka and M. Yamazaki, *Langmuir*, 2007, **23**, 720–728.
5 Y. Bashirzadeh and A. P. Liu, *Soft Matter*, 2019, **15**, 8425–8436.
6 T. Trantidou, L. Dekker, K. Polizzi, O. Ces and Y. Elani, *Interface Focus*, 2018, **8**, 20180024.
7 H. T. Hoang, M. Mertens, P. Wessig, F. Sellrie, J. A. Schenk and M. U. Kumke, *ACS Omega*, 2018, **3**, 18109–18116.
8 W. Zong, S. Ma, X. Zhang, X. Wang, Q. Li and X. Han, *J. Am. Chem. Soc.*, 2017, **139**, 9955–9960.
9 M. Weiss, J. P. Frohnmayer, L. T. Benk, B. Haller, J.-W. Janiesch, T. Heitkamp, M. Börsch, R. B. Lira, R. Dimova, R. Lipowsky, E. Bodenschatz, J.-C. Baret, T. Vidakovic-Koch, K. Sundmacher, I. Platzman and J. P. Spatz, *Nat. Mater.*, 2018, **17**, 89–96.
10 S. Deshpande and C. Dekker, *Emerging Top. Life Sci.*, 2019, **3**, 559–566.
11 S. Deshpande, W. K. Spoelstra, M. van Doorn, J. Kerssemakers and C. Dekker, *ACS Nano*, 2018, **12**, 2560–2568.
12 A. Booth, C. J. Marklew, B. Ciani and P. A. Beales, *iScience*, 2019, **15**, 173–184.
13 K. A. Ganzinger, A. Merino-Salomón, D. A. García-Soriano, A. Nelson Butterfield, T. Litschel, F. Siedler and P. Schwille, *bioRxiv*, 2019, 791459, DOI: 10.1101/791459.
14 S. Deshpande, F. Brandenburg, A. Lau, M. G. F. Last, W. K. Spoelstra, L. Reese, S. Wunnava, M. Dogterom and C. Dekker, *Nat. Commun.*, 2019, **10**, 1800.
15 L. L. A. Adams, T. E. Kodger, S.-H. Kim, H. C. Shum, T. Franke and D. A. Weitz, *Soft Matter*, 2012, **8**, 10719–10724.
16 J. P. Reeves and R. M. Dowben, *J. Cell. Physiol.*, 1969, **73**, 49–60.
17 A. Darszon, C. A. Vandenberg, M. Schönfeld, M. H. Ellisman, N. C. Spitzer and M. Montal, *Proc. Natl. Acad. Sci. U. S. A.*, 1980, **77**, 239.
18 M. I. Angelova and D. S. Dimitrov, *Faraday Discuss. Chem. Soc.*, 1986, **81**, 303–311.
19 H. Stein, S. Spindler, N. Bonakdar, C. Wang and V. Sandoghdar, *Front. Physiol.*, 2017, **8**, 63.
20 S. Pautot, B. J. Frisken and D. A. Weitz, *Langmuir*, 2003, **19**, 2870–2879.
21 J. C. Stachowiak, D. L. Richmond, T. H. Li, A. P. Liu, S. H. Parekh and D. A. Fletcher, *Proc. Natl. Acad. Sci. U. S. A.*, 2008, **105**, 4697–4702.
22 S. Deshpande and C. Dekker, *Nat. Protoc.*, 2018, **13**, 856–874.
23 L. R. Arriaga, S. S. Datta, S.-H. Kim, E. Amstad, T. E. Kodger, F. Monroy and D. A. Weitz, *Biophys. J.*, 2014, **106**, 42a.

24 B. Haller, K. Göpfrich, M. Schröter, J.-W. Janiesch, I. Platzman and J. P. Spatz, *Lab Chip*, 2018, **18**, 2665–2674.
25 K. Karamdad, R. V. Law, J. M. Seddon, N. J. Brooks and O. Ces, *Lab Chip*, 2015, **15**, 557–562.
26 M. Abkarian, E. Loiseau and G. Massiera, *Soft Matter*, 2011, **7**, 4610–4614.
27 P. C. Hu, S. Li and N. Malmstadt, *ACS Appl. Mater. Interfaces*, 2011, **3**, 1434–1440.
28 S. Deshpande, Y. Caspi, A. E. C. Meijering and C. Dekker, *Nat. Commun.*, 2016, **7**, 10447.
29 N.-N. Deng, M. Yelleswarapu and W. T. S. Huck, *J. Am. Chem. Soc.*, 2016, **138**, 7584–7591.
30 N.-N. Deng, M. A. Vibhute, L. Zheng, H. Zhao, M. Yelleswarapu and W. T. S. Huck, *J. Am. Chem. Soc.*, 2018, **140**, 7399–7402.
31 S. Deshpande, A. Birnie and C. Dekker, *Biomicrofluidics*, 2017, **11**, 034106.
32 K. Al Nahas, J. Cama, M. Schaich, K. Hammond, S. Deshpande, C. Dekker, M. G. Ryadnov and U. F. Keyser, *Lab Chip*, 2019, **19**, 837–844.
33 M. Schaich, J. Cama, K. Al Nahas, D. Sobota, H. Sleath, K. Jahnke, S. Deshpande, C. Dekker and U. F. Keyser, *Mol. Pharmaceutics*, 2019, **16**, 2494–2501.
34 M. Schulz, A. Olubummo and W. H. Binder, *Soft Matter*, 2012, **8**, 4849–4864.
35 D. Y. Alakhova and A. V. Kabanov, *Mol. Pharmaceutics*, 2014, **11**, 2566–2578.
36 P. Bao, D. A. Paterson, P. L. Harrison, K. Miller, S. Peyman, J. C. Jones, J. Sandoe, S. D. Evans, R. J. Bushby and H. F. Gleeson, *Lab Chip*, 2019, **19**, 1082–1089.
37 M. Khan and S.-Y. Park, *Colloids Surf., B*, 2015, **127**, 241–246.
38 H.-G. Lee, S. Munir and S.-Y. Park, *ACS Appl. Mater. Interfaces*, 2016, **8**, 26407–26417.
39 X. Niu, D. Luo, R. Chen, F. Wang, X. Sun and H. Dai, *Opt. Commun.*, 2016, **381**, 286–291.
40 M. Khan and S.-Y. Park, *Sens. Actuators, B*, 2014, **202**, 516–522.
41 E. Bukusoglu, X. Wang, J. A. Martinez-Gonzalez, J. J. de Pablo and N. L. Abbott, *Adv. Mater.*, 2015, **27**, 6892–6898.
42 I. H. Lin, D. S. Miller, P. J. Bertics, C. J. Murphy, J. J. de Pablo and N. L. Abbott, *Science*, 2011, **332**, 1297.
43 D. S. Miller, X. Wang and N. L. Abbott, *Chem. Mater.*, 2014, **26**, 496–506.
44 D. A. Paterson, P. Bao, R. H. Abou-Saleh, S. A. Peyman, J. C. Jones, J. A. T. Sandoe, S. D. Evans, H. F. Gleeson and R. J. Bushby, *Langmuir*, 2020, **36**, 6436–6446.
45 A. M. Lowe and N. L. Abbott, *Chem. Mater.*, 2012, **24**, 746–758.
46 S. Sidiq, D. Das and S. K. Pal, *RSC Adv.*, 2014, **4**, 18889–18893.
47 J. Jeong, Z. S. Davidson, P. J. Collings, T. C. Lubensky and A. G. Yodh, *Proc. Natl. Acad. Sci. U. S. A.*, 2014, **111**, 1742.
48 K. A. Simon, P. Sejwal, R. B. Gerecht and Y.-Y. Luk, *Langmuir*, 2007, **23**, 1453–1458.
49 C. Peng and O. D. Lavrentovich, *Soft Matter*, 2015, **11**, 7257–7263.
50 K. Nayani, R. Chang, J. Fu, P. W. Ellis, A. Fernandez-Nieves, J. O. Park and M. Srinivasarao, *Nat. Commun.*, 2015, **6**, 8067.
51 Z. H. Al-Lawati, B. Alkhairalla, J. P. Bramble, J. R. Henderson, R. J. Bushby and S. D. Evans, *J. Phys. Chem. C*, 2012, **116**, 12627–12635.
52 N. Boden, R. J. Bushby, L. Ferris, C. Hardy and F. Sixl, *Liq. Cryst.*, 1986, **1**, 109–125.
53 J. Steinkühler, P. De Tillieux, R. L. Knorr, R. Lipowsky and R. Dimova, *Sci. Rep.*, 2018, **8**, 11838.
54 D. J. Edwards, J. W. Jones, O. Lozman, A. P. Ormerod, M. Sintyureva and G. J. T. Tiddy, *J. Phys. Chem. B*, 2008, **112**, 14628–14636.
55 V. R. Horowitz, L. A. Janowitz, A. L. Modic, P. A. Heiney and P. J. Collings, *Phys. Rev. E: Stat., Nonlinear, Soft Matter Phys.*, 2005, **72**, 041710.
56 N. Zimmermann, G. Jünnemann-Held, P. J. Collings and H.-S. Kitzerow, *Soft Matter*, 2015, **11**, 1547–1553.
57 N. H. Hartshorne and G. D. Woodard, *Mol. Cryst. Liq. Cryst.*, 1973, **23**, 343–368.
58 L. Joshi, S.-W. Kang, D. M. Agra-Kooijman and S. Kumar, *Phys. Rev. E: Stat., Nonlinear, Soft Matter Phys.*, 2009, **80**, 041703.
59 H.-S. Park, S.-W. Kang, L. Tortora, Y. Nastishin, D. Finotello, S. Kumar and O. D. Lavrentovich, *J. Phys. Chem. B*, 2008, **112**, 16307–16319.
60 R. H. Abou-Saleh, J. R. McLaughlan, R. J. Bushby, B. R. Johnson, S. Freear, S. D. Evans and N. H. Thomson, *Langmuir*, 2019, **35**, 10097–10105.
61 P. C. Mushenheim, J. S. Pendery, D. B. Weibel, S. E. Spagnolie and N. L. Abbott, *Proc. Natl. Acad. Sci. U. S. A.*, 2016, **113**, 5564.
62 D. M. Agra-Kooijman, G. Singh, A. Lorenz, P. J. Collings, H. S. Kitzerow and S. Kumar, *Phys. Rev. E: Stat., Nonlinear, Soft Matter Phys.*, 2014, **89**, 6.
63 M. M. Genkin, A. Sokolov, O. D. Lavrentovich and I. S. Aranson, *Phys. Rev. X*, 2017, **7**, 011029.
64 S. Zhou, O. Tovkach, D. Golovaty, A. Sokolov, I. S. Aranson and O. D. Lavrentovich, *New J. Phys.*, 2017, **19**, 055006.